

SEARCH FOR RESONANT DOUBLE HIGGS PRODUCTION WITH BBZZ  
DECAYS IN THE  $b\bar{b}\ell\ell\nu\bar{\nu}$  FINAL STATE IN pp COLLISIONS AT  $\sqrt{s} = 13$  TeV

by

Rami Kamalieddin

A DISSERTATION

Presented to the Faculty of  
The Graduate College at the University of Nebraska  
In Partial Fulfilment of Requirements  
For the Degree of Doctor of Philosophy

Major: Physics and Astronomy

Under the Supervision of Professor Ilya Kravchenko

Lincoln, Nebraska

May, 2019

SEARCH FOR RESONANT DOUBLE HIGGS PRODUCTION WITH BBZZ  
DECAYS IN THE  $b\bar{b}\ell\ell\nu\bar{\nu}$  FINAL STATE IN pp COLLISIONS AT  $\sqrt{s} = 13$  TeV

Rami Kamalieddin, Ph.D.

University of Nebraska, 2019

Advisers: Ilya Kravchenko

Since the discovery of the Higgs boson in 2012 by the A Toroidal LHC ApparatuS (ATLAS) and The Compact Muon Solenoid (CMS), most of the quantum mechanical properties that describe the long-awaited Higgs boson have been measured. Due to an impeccable work of the LHC, dozens of  $fb^{-1}$  of data have been delivered to both experiments. Finally, it became possible for analyses that have a very low cross section to observe rare decay modes of the Higgs boson, as was done successfully recently in ttH and VHbb channels. The only untouched territory is a double Higgs boson production. Data will not help us much either at the HL-LHC, the process will remain unseen even in the most optimistic scenarios, so one has to rely solely on new reconstruction methods as well as new analysis techniques. This thesis is addressing both goals. I have been blessed by an opportunity to work in the CMS electron identification group, where we have developed new electron identification algorithms. The majority of this thesis, however, will be devoted to the second goal of HL-LHC. We establish the techniques for the first ever analysis at the LHC that searches for the double Higgs production mediated by a heavy narrow-width resonance in the  $b\bar{b}ZZ$  channel:  $X \rightarrow HH \rightarrow b\bar{b}ZZ^* \rightarrow b\bar{b}\ell\ell\nu\bar{\nu}$ . The analysis searches for a resonant production of a Higgs boson pair in the range of masses of the resonant parent particle from 250 to 1000 GeV. Both spin scenarios of the resonance are considered: spin 0 (later called "graviton") and spin 2 (later called "radion"). In the absence of the

evidence of the resonant double Higgs boson production from the previous searches, we set upper confidence limits. When combined with other search channels, this analysis will contribute to the discovery of the double Higgs production and we would be able to finally probe the Higgs boson potential using its self-coupling.

“... a place for a smart quote!”

*Lenin, 1922.*

## ACKNOWLEDGMENTS

This will be a longgggg list!

---

## Table of Contents

---

<b>List of Figures</b>	vii
<b>List of Tables</b>	viii
<b>1 LHC and the CMS experiment</b>	1
1.1 Introduction . . . . .	1
1.2 The LHC . . . . .	4
1.2.1 The Magnets . . . . .	4
1.2.2 Radio Frequency System . . . . .	6
1.2.3 Vacuum System . . . . .	7
1.2.4 Powering . . . . .	8
1.2.5 Cryogenic system . . . . .	9
1.2.6 Beam dumping system . . . . .	11
1.2.7 Beam injection system . . . . .	12
1.2.8 LHC injection chain . . . . .	12
1.3 The CMS experiment . . . . .	13
1.3.1 The CMS challenging environment . . . . .	14
1.3.2 CMS coordinate system . . . . .	17

<b>Bibliography</b>	<b>17</b>
---------------------	-----------

<b>References</b>	<b>19</b>
-------------------	-----------

---

## List of Figures

---

1.1	Schematic layout of the LHC. . . . .	3
1.2	The cross section of the LHC dipole . . . . .	5
1.3	Cables of the dipole magnet . . . . .	6
1.4	RF cavities module. . . . .	6
1.5	Beam screen. . . . .	8
1.6	13 kA high-temperature superconducting current lead. . . . .	9
1.7	Cross section of the LHC tunnel . . . . .	10
1.8	LHC cryogenic states and the temperature scale. . . . .	11
1.9	LHC injection complex. . . . .	13
1.10	CMS experiment with all sub-detectors shown. . . . .	14
1.11	Coordinate system of the CMS detector . . . . .	18

---

**List of Tables**

---

## CHAPTER 1

---

### LHC and the CMS experiment

---

#### 1.1 Introduction

Large Hadron Collider (LHC) (see Fig. 1.1) is the most powerful particle accelerator that has ever been built. It is located at the border of the France and Switzerland, reutilising the tunnel used previously by the Large Electron Positron collider. The whole LHC story begins in 1977, when CERN director general Sir John Adams suggested that LEP tunnel can be reused to accommodate the future hadron collider of more than 3 TeV energies ???. At the 1984 ECFA-CERN workshop on a "Large Hadron Collider in the LEP Tunnel" ??, the plans for LHC were stated, where the primary ones were the BEH mechanism, Higgs boson, and the origin of masses of W and Z bosons. The parameters of the LHC machine were very ambitious: the centre-of-mass energy of 10 to 20 TeV, and a target luminosity of  $10^{33-34} \frac{1}{cm^2 s}$ . Luminosity is the coefficient which relates the cross section of the event under study to the number of events that will be generated in the LHC collision:  $N_{events} = L\sigma_{event}$ . Luminosity is the parameter control by the machine and for Gaussian beams ?? can be written as:

$$L = \frac{N_b^2 n_b f_{rev} \gamma_r}{4\pi \epsilon_n \beta^*} F$$

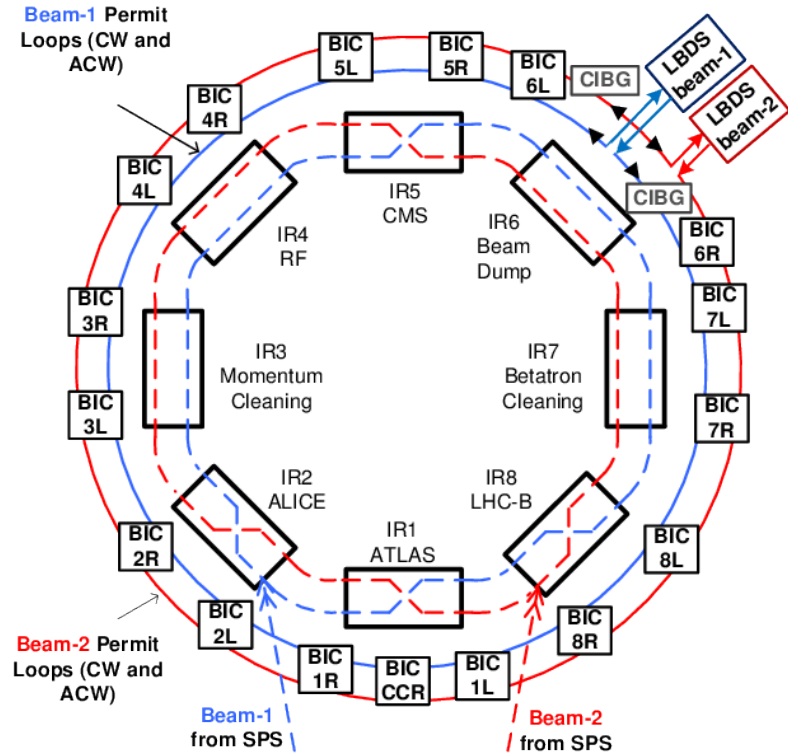
where  $N_b$  is the number of particle in the colliding bunch,  $n_b$  is the number of colliding

bunches in the beam,  $f_{rev}$  is the revolution frequency,  $\gamma_r$  is the relativistic factor,  $\varepsilon_n$  is the normalised transverse beam emittance,  $\beta^*$  is the beta function at the collision point, and  $F$  is the factor related to the crossing angle at the interaction point (IP). The luminosity is not constant and decays with time due to the degradation of the initial circulating beams. Decay time is approximately 45 h, and 29 h to reach  $1/e$  level. Adding contribution from the intrabeam scattering, scattering on the residual gas, etc, the final luminosity lifetime is about 15 h.

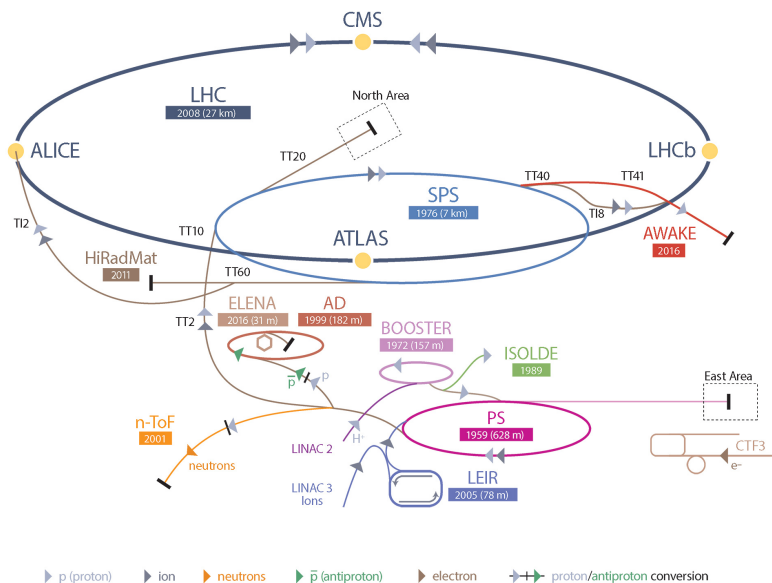
Another useful variation of the luminosity parameter is an integrated luminosity. Integrating over the yield of a single run we get:

$$L_{int} = L_0 \tau_L \left[ 1 - e^{-\frac{T_{run}}{\tau_L}} \right],$$

where  $L_0$  is the initial luminosity,  $T_L$  is the total length of the run, and  $\tau_L$  is the luminosity lifetime. The optimum runtime thus is either 5.5 or 12 hours, which potentially leads to  $80 - 120/fb$  of data with barn  $b$  denoting a unit area of  $10^{28} m^2$ .



CERN's Accelerator Complex

**Figure 1.1:** Schematic layout of the LHC.

## 1.2 The LHC

The first LHC budget plan was approved in 1996 and the final cost sum was completed in 2008. 4 years later the Higgs discovery happened, in 2012, quite fast for such a huge project! Now we will talk about the most important parts of the LHC complex one-by-one. Let us start with magnets.

### 1.2.1 The Magnets

To keep the beam of protons on a circular orbit LHC needs strong magnets. The proven technology existed since Tevatron and relied on  $NbTi$  superconductors. 1232 dipoles at  $8\text{ }T$ , which are cooled to the below  $2\text{ }K$  temperature using superfluid Helium, bend the beam 1.2. The dipole cold mass is in the so-called Helium bath and is cooled down to  $1.9\text{ }K$ . Each of the  $16.5\text{ }m$  (with ancillaries) long and  $570\text{ }mm$  in diameter dipoles is slightly curved by  $5.1\text{ }mrad$  to help a chain of dipoles complete 360 degrees. The dipole is located inside of the dipole cryostat, which is a long cylindrical tube  $914\text{ }mm$  in diameter made of low-carbon steel. During the standard operation time the vessel contains the vacuum.

## LHC DIPOLE : STANDARD CROSS SECTION

CERN AC/DI/MM - HE107 - 30 04 1999

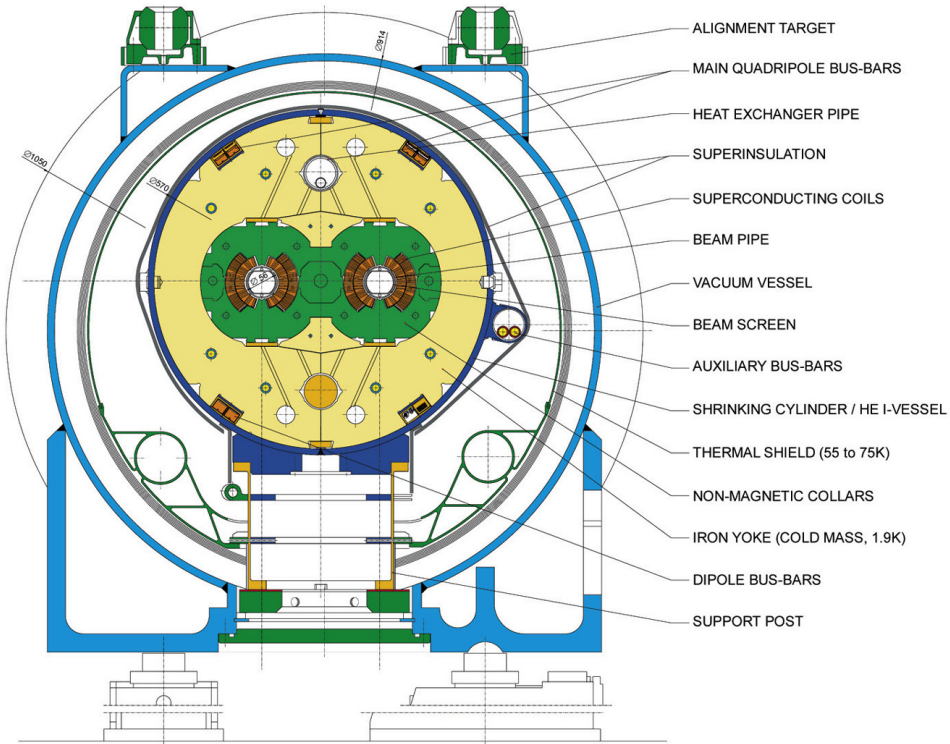


**Figure 1.2:** The cross section of the LHC dipole.

The material and the properties of the cables for the dipoles had to be carefully chosen. Each dipole coil is 56 mm in diameter and is made of cables of two types. The cable in the inner layer contains 28 strands 1.065 mm each. The outer layer contains 36 strands 0.825 mm each 1.3.

To correct the orbit, higher order correctors are used with about 3800 single aperture and 1000 twin aperture magnets evenly spaced around the circular trajectory.

Another important task that is performed with the use of magnets is the beam insertion, which is done at eight specific insertion locations. LHC also uses *NbTi* magnets to accomplish this work.

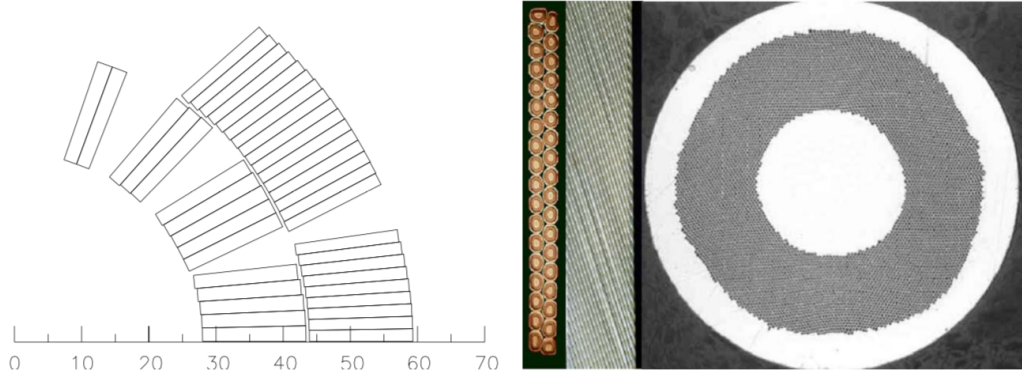


**Figure 1.3:** Cables of the dipole magnet. Left: cross section view. Right: Strand and cables

### 1.2.2 Radio Frequency System

The beam that comes from injectors will be placed, accelerated and kept on the orbit with the help of Radio Frequency (RF) cavities (see Fig. 1.4). The same system will be used to correct for injection errors in the beam direction. RF will be operating at the  $400\text{ MHz}$ , which is 10 times more than the revolution frequency of  $40\text{ MHz}$ .

Four RF cavities grouped together into one cryomodule constitute an important accelerating module. If something happens to this module, it can be easily replaced in short period of time.

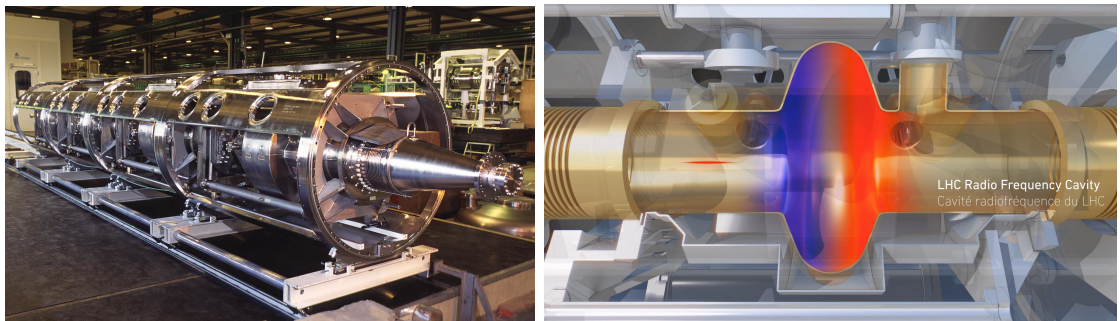


**Figure 1.4:** LHC RF cavities. Left: a cryomodule with four RF cavities. Right: a single RF cavity schematic drawing. The colour field is used to highlight the fact of two field of the different polarity.

### 1.2.3 Vacuum System

Three types of vacuum systems are necessary for the LHC proper operation. The vacuum system for the cryomagnets, the insulation vacuum for helium distribution, and, of course, the vacuum for the beam (VBS). As a convention, taking into account ionisation cross sections for gasses of the interests, cryogenic temperatures are expressed as corresponding gas densities normalised to the hydrogen. VBS, to ensure the 100 hours long run time, requires the equivalent hydrogen densities (EHD) to be below  $10^{15} H_2 \frac{1}{m^3}$ . To minimise the backgrounds from the experiments, the EHD at the interaction points should be  $10^{13} H_2 \frac{1}{m^3}$ . Those parts of the beam system, which operate under room temperatures, are under the pressure of  $10^{-10}$  to  $10^{-11}$  mbar. All the vacuum section are subdivided into smaller modules to allow easy repair and fine tuning. VBS, as the most demanding in terms of the vacuum quality, have to be properly designed and must address a number of challenges, such as synchrotron radiation that significantly affects vacuum chambers in the arcs around the tunnel, as well as an electron cloud effect which exists along the length of the whole circle of the LHC. After the beam is inserted and is stabilised, the final adjustment of the VBS is needed to guarantee the perfect performance.

To finish the discussion of the VBS, let us discuss which heat sources have the main effect on the vacuum of the beam that must exist at the 1.9 K.

- Synchrotron radiation ( $0.2 W/m$  per beam)
- Energy loss by nuclear scattering ( $30 mW/m$  per beam)
- Image currents ( $0.2 W/m$  per beam)
- Electron cloud related effects (vary)

To obstruct the heat sources mentioned above, specific beam screens are developed (see Fig. 1.5). Screens have elliptical shape, so-called racetrack shape, which gives extra space for cooling while optimises the aperture. Finally, the lifetime of the vacuum is mostly determined by the interactions of the vacuum gas nuclei with the protons of the beam. Values of the cross sections of such processes are given in ??.

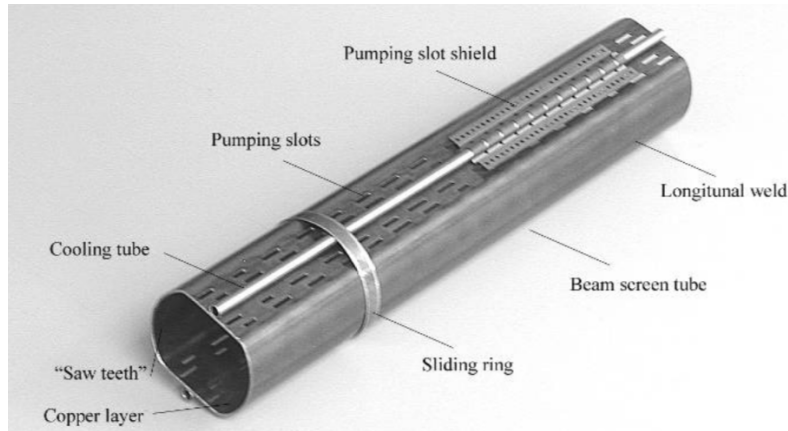


**Figure 1.5:** Beam screen.

#### 1.2.4 Powering

To power the LHC, 1612 electrical circuits of 131 types are used. The magnets are powered in eight symmetrical sections. Some sections rely on all 131 types of circuits, while others may use only specific ones. To power the main quadrupoles which focus the beam, the power converters are located in the underground area. A total of 3286 current leads is needed to connect all the circuits and power cables. 1070 of the leads operate between 600 A and 13 kA (see Fig. 1.6). The other leads work in the range 60 to 120 A.



**Figure 1.6:** 13 kA high-temperature superconducting current lead.

### 1.2.5 Cryogenic system

The cryogenic system (see Fig. 1.7) must supply the LHC cold mass of 37 Mkg within 15 days with the necessary temperature settings and work with the temperatures different by 75 K. The system must also be able to deal with the fast pressure raises and flow surges, and should be able to recover in a short period of time from such perturbations not to affect the run of the whole LHC. Another important point during the cryogenic design that had to be addressed is the fact that the LHC tunnel is

inclined in the horizontal plane by 1.41 °. This equals to 120 m difference in the vertical location of two diametrically opposite points of the tunnel with respect to the surface level and results in the additional hydrostatic pressure that can affect the flow of the cryogen. To avoid any instability of the LHC work like this, the gas is transported in the super-heated-vapour state.

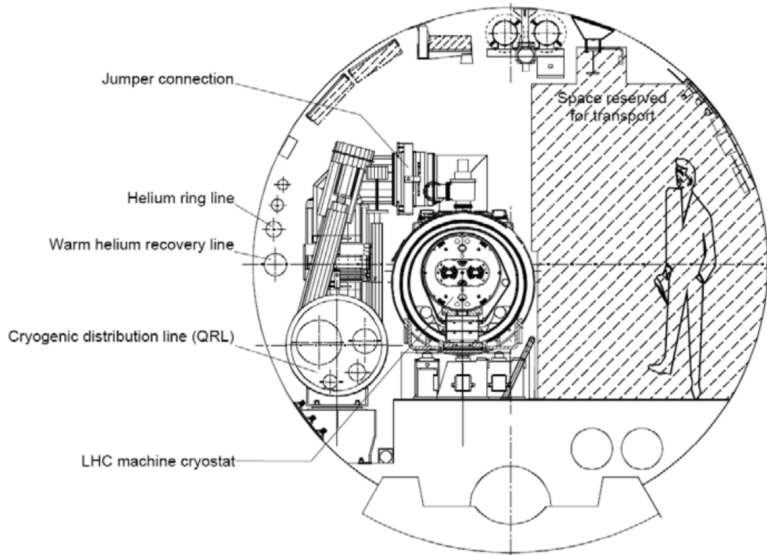


**Figure 1.7:** Cross section of the LHC tunnel

Since the cost of the production of 1.8 K temperature is high, several temperature levels are employed (see Fig. 1.8):

- 50 to 75 K for the thermal shielding that protects the cold masses
- 4.6 to 20 K for lower temperature interception and to cool the beam screens
- 1.9 K for quasi-isothermal helium in the superfluid state to cool the magnet cold mass
- 4 K for the transportation system that directs the 1.8 K helium from the exchanger to the 1.8 K refrigerator

- 4.5 K for RF cavities and lower sections of the high-temperature superconducting current leads
- 20 to 300 K for upper sections of the high-temperature superconducting current leads

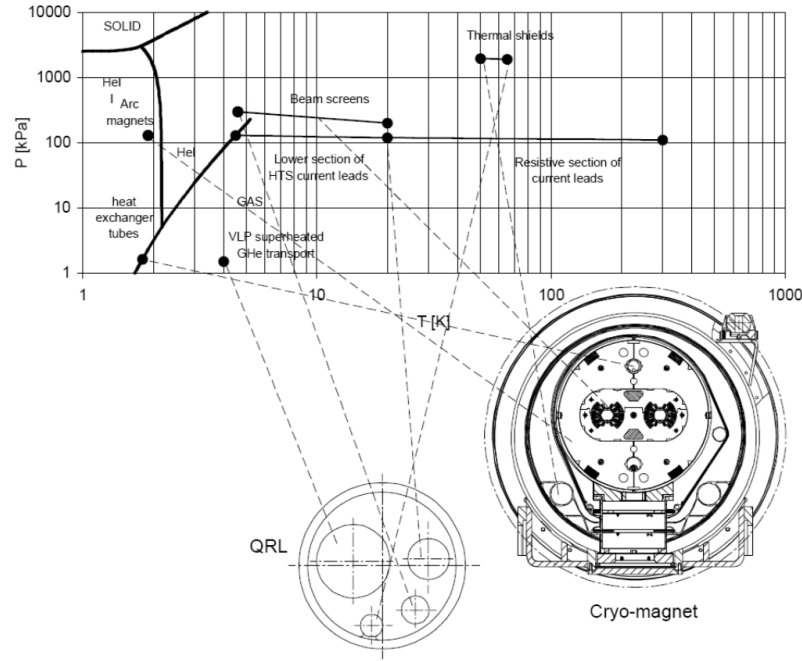


**Figure 1.8:** LHC cryogenic states and the temperature scale.

### 1.2.6 Beam dumping system

The LHC beam carries a lot of power and a well-designed and reliable beam extraction and dumping system is needed. Point 6 at LHC contains such system, which is able to fast-extract the beam in a loss-free way. The system for each ring comprises:

- 15 kicker magnets for extraction
- 15 steel septum magnets around the Point 6 interaction point
- 10 modules of the dilution kicker magnets

- the beam dump proper with the associated steel and concrete for shielding
- dedicated dilution devices

### **1.2.7 Beam injection system**

The injection at LHC is done at two points and for two beams separately: at Point 2 and Point 8. The beam comes to the insertion point from outside and below the machine level. A series of magnets and a kicker then deflects the beam horizontally and vertically to place the beam on the LHC orbit. To protect against the problematic injections and malfunctioning of the kickers, a series of the collimators correct the incoming beam.

### **1.2.8 LHC injection chain**

To place the beam at the final LHC orbit, the protons from the hydrogen bottle extracted from the hydrogen gas have to travel a long pass during which they are put into bunches and accelerated to the nominal collision speed.

## The LHC injection complex

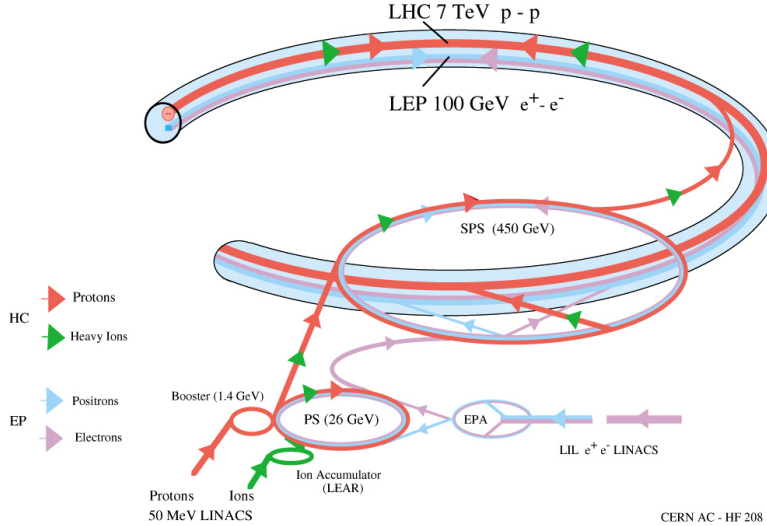


Figure 1.9: LHC injection complex.

The accelerator complex consists of: LINAC, Booster, Proton Synchrotron, Super Proton Synchrotron, and finally, the LHC main ring (see Fig. 1.9).

The whole LHC complex has to satisfy requirements of the final ring, such as:

- the beam emittance has to be compatible with the small aperture of the LHC superconducting magnets
- the effect of the synchrotron radiation has to be taken into account when calculating the required cryogen needs for the intensity of the incoming beam
- the beam-beam interactions that enhance the betatron oscillations
- in the injector the space-charge limits have to be taken into account

## 1.3 The CMS experiment

The total inelastic cross section of the proton-proton interaction at  $\sqrt{s} = 14$  TeV will be about 100 mb. The detectors observe the event rate of nearly  $10^9$  inelastic

events per second. This flow of data is too large to be stored, and also, does not contain that many event of interest. Therefore, the trigger system must reduce the event rate to manageable 100 events per second. In addition, a pile up (PU) of 20-200 events overlaid with the event of interest will be expected, which results in about 1000 particles produced every 25 ns. All sub-detectors of CMS (see Fig. 1.10), thus, have to be able to work fast and in a good synchronisation with each other.

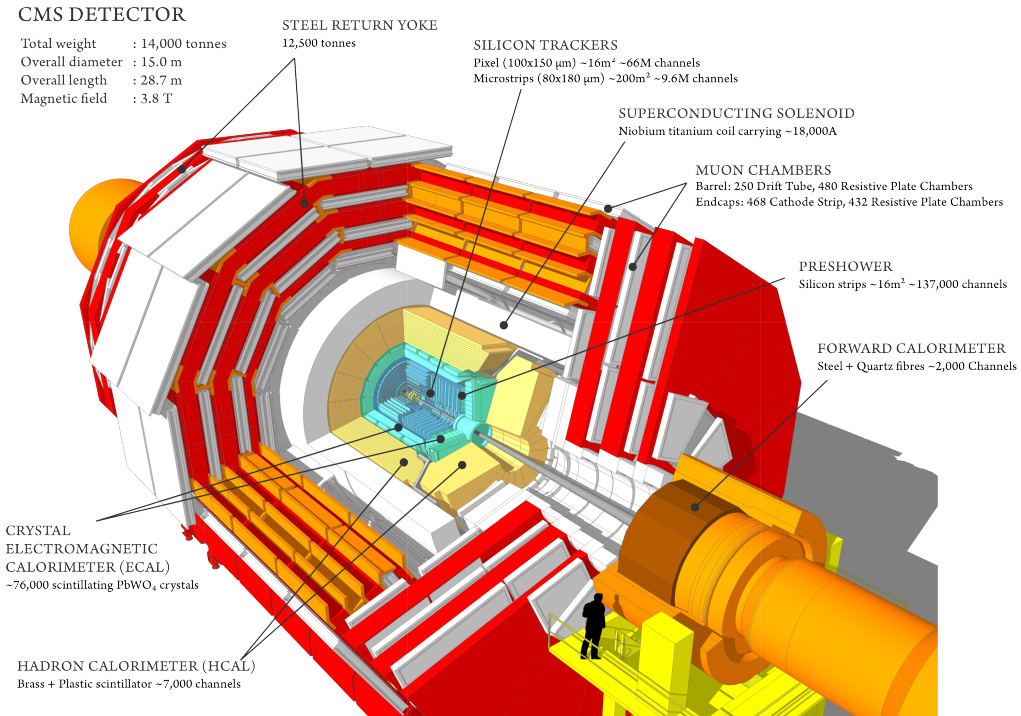


**Figure 1.10:** CMS experiment with all sub-detectors shown.

### 1.3.1 The CMS challenging environment

One can summarise all challenges and requirements that the CMS has faced in the following list:

- good muon momentum resolution over the momentum scale covering almost a TeV range, good dimuon resolution at the 100 GeV, and a capability to de-

termine correctly the charge of the highly energetic muon all the way up to 1 TeV

- good momentum resolution of the charged particles in the inner tracker. Emphasis on the efficient  $\tau$  lepton and b-jets reconstruction
- good performance of the electromagnetic calorimeter (ECAL), with the particular attention to the diphoton mass resolution, ability to reject efficiently  $\pi^0$ , ability to identify isolated photons and leptons
- good missing transverse mass and dijet-mass resolution, which depends heavily on the performance of the hadronic calorimeter (HCAL)

The CMS design has been driven by the needs to have a large bending power, which is to be provided by the superconducting magnet, to be able to disentangle among each other various charged particles. The size of the magnet is 13 m in length and 6 m in inner diameter. 4 T solenoid provides 12 Tm bending power. The inner diameter is large enough to host the inner tracker and the ECAL. To address the high multiplicity problem, the CMS inner tracker uses 10 layers of the silicon microstrip detectors. The inner barrel contains four layers of strips and the outer barrel has six layers. Each silicon sensor is  $320 \mu m$  in height and a specifically designed overlay of strips provides a spatial resolution of  $13\text{-}38 \mu m$ . About the same resolution is achieved by the other tracker. The whole tracker contains 15148 silicon modules with the 9.3 million strips. Tracker provides the experiments with the tracks information left by the charged particles traversing its material.

To further improve the impact parameter determination and secondary vertex reconstruction, three layers of the silicon pixel detector are inserted near the interaction

region. Pixel detector is composed of 1440 silicon pixel detector modules organised in three concentric cylindrical layers, and also two disks in the forward regions.

The ECAL technology is based on the on the lead tungstate crystals ( $PbWO_4$ ). The ECAL measures the energy deposited by photons and electrons. ECAL contains 75848 crystals where the energy showers will be produced by the particles releasing their energy when interacting with the material of the crystals. Before the ECAL, a preshower system is placed to reject  $\pi^0$ . It contains layers of lead radiators followed by layers of the silicon strips to initiate and subsequently to measure the energy of the particle. The ECAL measured energy of the particles is a function of the stochastic term (S), noise (N), and a constant term (C).

$$\left(\frac{\sigma}{E}\right)^2 = \left(\frac{S}{\sqrt{E}}\right)^2 + \left(\frac{N}{E}\right)^2 + C^2 \quad (1.1)$$

The ECAL is surrounded by the HCAL system which is based on the brass/scintillator sampling hadronic technology. HCAL measures energy of particles made of quarks. Central part is later covered by the *tail-catcher* leaving 11 hadronic interaction lengths to the particle interactions. Further, the forward calorimeter is used to ensure the coverage in  $\eta$  up to 5. Note, that the coverage of ECAL and HCAL are about up to  $\eta = 3$ .

Additional dedicated detectors such as CASTOR, ZDC, etc, ensure that the detector has a full  $4\pi$  coverage. HCAL does not fully absorb energy of the the particles traversing its medium, except very low energy particles, thus the energy of the particles is sampled to estimate the total amount.

Overall, the CMS detector is 21.6 m in length and 14.6 m in diameter. The weight of the whole construction is near 12 500 tons. ECAL covers more than 25 radiation lengths, HCAL, from 7 to 11, depending on the  $\eta$  region. Outer HCAL is located

outside of the magnet.

The superconducting magnet of CMS provides the experiment with almost 4 T magnetic field and is operated at the 4.7 K temperature. Additionally, a magnet yoke is made of five barrel wheels is used for the magnetic flux return and serves as a support for the embedded muon system, which is located outside of the ECAL and HCAL systems. Muons are energetic enough to traverse the ECAL and leave the detector. Tracks in the muon system will be used to reconstruct standalone muons, and in combination with the tracker, to reconstruct the global muons.

### 1.3.2 CMS coordinate system

It is useful to introduced a convenient coordinates system used by the CMS experiment. We will use rapidity and pseudorapidity many times in the analysis section of the thesis. The coordinate system employed by the CMS uses the rapidity,  $y$ , and pseudorapidity,  $\eta$ . They are derivatives of the log functions of the energy and a projection of the momentum on the  $z$  axis and the angle  $\theta$  with respect to the beam axis (see Fig. 1.11 ??):

$$y = \frac{1}{2} \ln \frac{E + p_z}{E - p_z} \quad \eta = -\ln \left( \tan \frac{\theta}{2} \right) \quad (1.2)$$

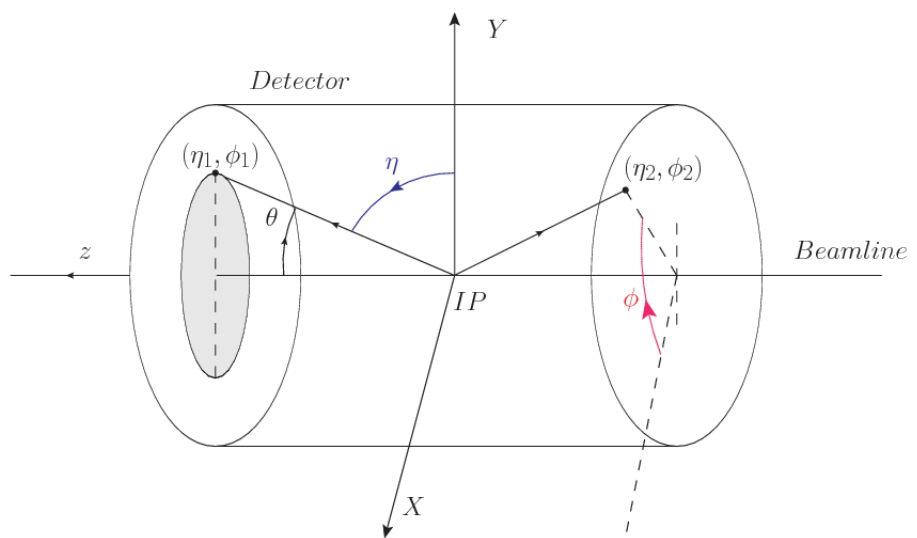


**Figure 1.11:** Coordinate system of the CMS detector.

---

## References

---

- [1] Matthias U. Mozer. Electroweak Physics at the LHC. *Springer Tracts Mod. Phys.*, 267:1–115, 2016.
- [2] Gennadi Sardanashvily. *Noether’s theorems: applications in mechanics and field theory*. Atlantis studies in variational geometry. Springer, Paris, 2016.
- [3] Steven Weinberg. The Making of the Standard Model. *Eur. Phys. J. C*, 34(hep-ph/0401010):5–13. 21 p. ; streaming video, 2003.
- [4] Roger Wolf. *The Higgs Boson Discovery at the Large Hadron Collider*, volume 264. Springer, 2015.
- [5] Jose Andres Monroy Montanez, Kenneth Bloom, and Aaron Dominguez. Search for production of a Higgs boson and a single Top quark in multilepton final states in pp collisions at  $\sqrt{s} = 13$  TeV, Jul 2018. Presented 23 Jul 2018.
- [6] Peisi Huang, Aniket Joglekar, Min Li, and Carlos E. M. Wagner. Corrections to di-Higgs boson production with light stops and modified Higgs couplings. *Phys. Rev.*, D97(7):075001, 2018.
- [7] Matthew J. Dolan, Christoph Englert, and Michael Spannowsky. New Physics in LHC Higgs boson pair production. *Phys. Rev.*, D87(5):055002, 2013.

- [8] Shinya Kanemura, Kunio Kaneta, Naoki Machida, Shinya Odori, and Tetsuo Shindou. Single and double production of the Higgs boson at hadron and lepton colliders in minimal composite Higgs models. *Phys. Rev.*, D94(1):015028, 2016.
- [9] Albert M Sirunyan et al. Search for Higgs boson pair production in the  $\gamma\gamma b\bar{b}$  final state in pp collisions at  $\sqrt{s} = 13$  TeV. 2018.
- [10] Alexandra Oliveira. Gravity particles from Warped Extra Dimensions, predictions for LHC. 2014.
- [11] Lisa Randall and Raman Sundrum. A Large mass hierarchy from a small extra dimension. *Phys. Rev. Lett.*, 83:3370–3373, 1999.
- [12] Kunihiro Uzawa, Yoshiyuki Morisawa, and Shinji Mukohyama. Excitation of Kaluza-Klein gravitational mode. *Phys. Rev.*, D62:064011, 2000.
- [13] H. Davoudiasl, J. L. Hewett, and T. G. Rizzo. Phenomenology of the Randall-Sundrum Gauge Hierarchy Model. *Phys. Rev. Lett.*, 84:2080, 2000.
- [14] Michael Forger and Hartmann Romer. Currents and the energy momentum tensor in classical field theory: A Fresh look at an old problem. *Annals Phys.*, 309:306–389, 2004.
- [15] Chuan-Ren Chen and Ian Low. Double take on new physics in double Higgs boson production. *Phys. Rev.*, D90(1):013018, 2014.
- [16] Roberto Contino, Margherita Ghezzi, Mauro Moretti, Giuliano Panico, Fulvio Piccinini, and Andrea Wulzer. Anomalous Couplings in Double Higgs Production. *JHEP*, 08:154, 2012.

- [17] Richard Phillips Feynman, Robert Benjamin Leighton, and Matthew Sands. *The Feynman lectures on physics; New millennium ed.* Basic Books, New York, NY, 2010. Originally published 1963-1965.
- [18] Savas Dimopoulos, Stuart Raby, and Frank Wilczek. Proton decay in supersymmetric models. *Physics Letters B*, 112(2):133 – 136, 1982.
- [19] David J Griffiths. *Introduction to elementary particles; 2nd rev. version.* Physics textbook. Wiley, New York, NY, 2008.
- [20] M. Della Negra, P. Jenni, and T. S. Virdee. Journey in the search for the higgs boson: The atlas and cms experiments at the large hadron collider. *Science*, 338(6114):1560–1568, 2012.
- [21] Jennifer Ouellette. Einstein’s quest for a unified theory. *APS*, 2015.
- [22] E A Davis and Isabel Falconer. *J.J. Thompson and the discovery of the electron.* Taylor and Francis, Hoboken, NJ, 2002.
- [23] Oreste Piccioni. *The Discovery of the Muon*, pages 143–162. Springer US, Boston, MA, 1996.
- [24] G. Danby, J-M. Gaillard, K. Goulian, L. M. Lederman, N. Mistry, M. Schwartz, and J. Steinberger. Observation of high-energy neutrino reactions and the existence of two kinds of neutrinos. *Phys. Rev. Lett.*, 9:36–44, Jul 1962.
- [25] M. L. Perl, G. S. Abrams, and et al Boyarski. Evidence for anomalous lepton production in  $e^+ - e^-$  annihilation. *Phys. Rev. Lett.*, 35:1489–1492, Dec 1975.
- [26] K. Kodama et al. Observation of tau neutrino interactions. *Phys. Lett.*, B504:218–224, 2001.

- [27] S. M. Bilenky. Neutrino in Standard Model and beyond. *Phys. Part. Nucl.*, 46(4):475–496, 2015.
- [28] S Chandrasekhar. *Newton's principia for the common reader*. Oxford Univ., Oxford, 2003. The book can be consulted by contacting: PH-AID: Wallet, Lionel.
- [29] Hanoch Gutfreund and Jürgen Renn. *The road to relativity: the history and meaning of Einstein's "The foundation of general relativity" : featuring the original manuscript of Einstein's masterpiece*. Princeton University Press, Princeton, NJ, Apr 2015.
- [30] J. Butterworth. *Smashing Physics*. Headline Publishing Group, 2014.
- [31] W N Cottingham and D A Greenwood. *An Introduction to the Standard Model of Particle Physics; 2nd ed.* Cambridge Univ. Press, Cambridge, 2007.
- [32] Eric W. Weisstein. Fundamental forces.
- [33] Carl Bender. Mathematical physics.
- [34] Andrew Wayne. QED and the Men Who Made It: Dyson, Feynman, Schwinger, and Tomonaga by Silvan S. Schweber. *The British Journal for the Philosophy of Science*, 46(4):624–627, 1995.
- [35] C. Patrignani et al. Review of Particle Physics. *Chin. Phys.*, C40(10):100001, 2016.
- [36] Michelangelo L Mangano. Introduction to QCD. (CERN-OPEN-2000-255), 1999.
- [37] Matt Strassler. Of particular significance: Conversations about science with theoretical physicist matt strassler.

- [38] S. L. Glashow. Partial Symmetries of Weak Interactions. *Nucl. Phys.*, 22:579–588, 1961.
- [39] F. Englert and R. Brout. Broken symmetry and the mass of gauge vector mesons. *Phys. Rev. Lett.*, 13:321–323, Aug 1964.
- [40] Peter W. Higgs. Broken symmetries and the masses of gauge bosons. *Phys. Rev. Lett.*, 13:508–509, Oct 1964.
- [41] G. S. Guralnik, C. R. Hagen, and T. W. B. Kibble. Global conservation laws and massless particles. *Phys. Rev. Lett.*, 13:585–587, Nov 1964.
- [42] Pauline Gagnon. *Who cares about particle physics? : making sense of the Higgs boson, the Large Hadron Collider and CERN*. Oxford University Press, 2016.